Mapping Soil Erosion in a Quaternary Catchment in Eastern Cape Using Geographic Information System and Remote Sensing

Kwanele Phinzi[a]*, Njoya Silas Ngetar[a]

[a]School of Agricultural, Earth and Environmental Sciences, Discipline of Geography, University of KwaZulu-Natal, Durban, South Africa

*Corresponding author's email: kwanelep48634@gmail.com.

DOI: http://dx.doi.org/10.4314/sajg.v6i1.2

Abstract

In South Africa, soil erosion is considered as an environmental and social problem with serious financial implications particularly in some rural areas where this geomorphological phenomenon is widespread. An example is the Umzimvubu Local Municipality, where most households are strongly reliant on agriculture for their livelihood. Sustainable agriculture and proper land management in these rural areas require information relevant to the spatial distribution of soil erosion. This study was therefore aimed at generating such information using Landsat8 Operational Land Imager (OLI)-derived vegetation indices (VIs) including the Normalised Difference Vegetation Index (NDVI), Soil Adjusted Vegetation Index (SAVI), as well as Soil and Atmospherically Resistance Vegetation Index (SARVI). Raster calculator in ArcMap10.2 was used to classify soil erosion features based on selected suitable thresholds in each VI. SPOT6/7 (Satellites Pour l'Obsevation de la Terre) multispectral data and Google Earth images were used for ground truth purposes. SAVI achieved the highest overall classification accuracy of 83% and kappa statistics of 64%, followed by NDVI and SARVI with equal overall accuracy of 81% and slightly different kappa statistics of 60% for the former and 59% for the latter. Using these indices, the study successfully mapped the spatial distribution of soil erosion within the study area albeit there were some challenges due to coarser spatial resolution (15mx15m) of Landsat8 image. Due to this setback, image fusion and pan-sharpening of Landsat8 with higher spatial resolution images is strongly suggested as an alternative to improve the Landsat8 spatial resolution.

Keywords: Geographic Information System; Remote Sensing; Soil Erosion; Vegetation Indices

1. Introduction

Soil erosion is considered one of the world's most critical environmental concerns owing to its adverse effects on both the natural environment and human society (Jie *et al*., 2002; Le Roux *et al*., 2008; Aiello *et al*., 2015). Globally, approximately 2 billion hectares (22 percent) of all cropland, pasture, forest and woodland around the world have been degraded since last century (Oldeman *et al*., 1991; Scherr and Yadav, 1997; Pimentel, 2006). In financial terms, according to Scherr (1999) cited in Jie *et al*. (2002), at least $28 billion have been lost per year due to soil degradation in drylands around the world. While soil erosion affects both the developed and developing world, the latter appears to have experienced more severe erosion than its developed counterpart. In South Africa, more than 70% of the land is subject to significant levels of soil erosion (Garland *et al*., 2000). Many soil erosion-borne studies (including Beckedhal and De Villiers, 2000; Boardman *et al*., 2003; Ngetar, 2011) have been conducted over the past few years in South Africa. However, one weakness of the South African soil erosion research is the limited information on where the problem is highly concentrated (Le Roux *et al*., 2007). Considerable attention has been paid to the "what" question rather than to the "where" question and this calls for more research to generate adequate information regarding the spatial distribution of the problem.

Studies making use of geospatial technologies including GIS and remote sensing to map the spatial distribution of soil erosion in South Africa are relatively recent (Le Roux and Sumner, 2012; Seutloali *et al*., 2015). For example, Mararakanye and Nethengwa (2012) mapped the spatial distribution of gully erosion in Limpopo using remote sensing and traditional techniques. Le Roux and Sumner (2012) also digitised continuous and discontinuous gullies from SPOT5 imagery showing the spatial extent of gullies at a catchment scale. More recently, using Landsat multispectral data, Seutloali *et al*. (2016) produced soil erosion severity index maps of the former homelands of Transkei. Despite the use of GIS and remote sensing in soil erosion studies in South Africa, there is still a need to map the spatial extent of the problem (Le Roux *et al*., 2007) in other erosion-prone areas such as the Umzimvubu Municipality (Eastern Cape) within which the study area (catchment) falls. Dissemination of information relevant to the spatial distribution of soil erosion within the municipality is critical to land conservation and management. If governance is about decision-making, then up-to-date, accurate, complete and usable information on soil erosion is indispensable to governance (Macharia, 2005) at a local level, namely, the municipality. However, this requires the availability of high spatial resolution imagery. In the absence of such imagery, freely available coarse resolution imagery can be used to provide an insight into the nature of soil erosion in an area.

Different techniques exist for the assessment of soil erosion phenomenon including the most widely used Universal Soil Loss Equation (USLE) developed by Wischmeier and Smith (1965). The use of USLE and its enhanced versions have been instrumental in estimating soil loss rates with reasonable costs and better accuracy especially when combined with GIS and remotely sensed data (Owusu, 2012; Alexakis *et al*., 2013; Ganasri and Ramash, 2015). Nonetheless, as highlighted by Merritt *et al*. (2003) and Kinnell (2010), USLE (including its enhanced versions) was designed to assess rill and inter-rill erosion and hence its application is problematic in areas where ephemeral and classical gullies are dominant forms. Besides this apparent limitation, USLE or any other soil loss model is not considered in this paper since the paper is primarily concerned with the spatial distribution of the erosion phenomenon as opposed to modelling absolute values of soil loss. Various remote sensing techniques (automated and semi-automated) exist for mapping soil erosion, ranging from pixel-based to object-oriented image classification with the latter relying on fine spatial resolution images. While the growing availability of high spatial resolution images such as IKONOs, QuickBird, and WorldView has facilitated a shift from traditional pixel-based to object-based methods (Shruthi *et al*., 2011; Mayr *et al*., 2016), these images are not readily or freely available. Additionally, such high spatial resolution images have limited spectral bands as noted by Taruringa (2008) and Shruthi *et al*. (2011). It is therefore not surprising that medium resolution images such as Landsat still appeal to some soil erosion researchers (Seutloali *et al*., 2016; Dube *et al*., 2017).

The use of semi-automated image classification techniques such as vegetation indices (VIs) in particular have gained momentum in soil erosion research over the past few decades (Mathieu *et al*., 1997; Singh, 2004). Since its introduction in the 1970s by Rouse *et al*. (1973), the Normalised Difference Vegetation Index (NDVI) has been used quite extensively in soil erosion-related research (Vaidyanathan *et al*., 2002; Li *et al*., 2010; Seutloali *et al*., 2016). However, the extensive use of NDVI has also presented significant weaknesses. Govaerts and Verhulst (2010) note that satellite-based NDVI results are subject to interference by non-vegetation factors including, but not limited to atmospheric conditions and soil background. Consequently, various modifications have been proposed to address the sensitivity of NDVI to non-vegetation factors (Lawrence and Ripple, 1998). The Soil Adjusted Vegetation Index (SAVI) proposed by Huete (1988), and Soil and Atmospherically Resistant Vegetation Index (SARVI) developed by Huete and Liu (1994) are amongst the most widely used modifications of NDVI in soil erosion research.

In this paper, satellite image-derived NDVI, SAVI, and SARVI are considered mainly because they are some of the simplest, cheapest, and quickest feature extraction techniques (Singh, 2004;

Gandhi *et al*., 2015; Alhawiti and Mitsova, 2016; Sonawane and Bhagat, 2017) that can be used to map soil erosion events. Soil erosion is a dynamic process requiring constant monitoring while keeping up-to-date information on its spatial distribution. However, in the study area and the case of Umzimvubu Municipality at large, existing information on soil erosion (Madikizela, 2000) is out-dated and sparse. Apparently, there are no soil erosion studies in the area which have taken advantage of GIS and remote sensing and their assessment methods, particularly the use of VIs. Therefore, the main objective of this study is twofold: (1) to map the spatial distribution of soil erosion in the study area using three Landsat-derived VIs, namely; NDVI, SAVI, and SARVI, and (2) to assess the accuracy of VI-derived soil erosion maps and determine the best VI for detecting soil erosion features at a catchment level.

2. Description of the Study Area

The study area constitutes one of the most severely eroded catchments in the Eastern Cape and is located in the central part of Umzimvubu Local Municipality. It includes sections of the Matatiele and Ntabankulu local municipalities on the north and south, respectively. The approximate geographic coordinates of the catchment area are 30° 38´ 23.5´´- 30° 55´ 29.50´´ S and 28° 42´ 36.65´´ - 29° 10´ 19.17´´ E (Figure 1), and covers approximately 503km² of the total municipal surface area (2 506km²). The study area exhibits a highly uneven topography with an elevation range of 820m to 1970m above sea level, for low-lying and high-lying areas, respectively.

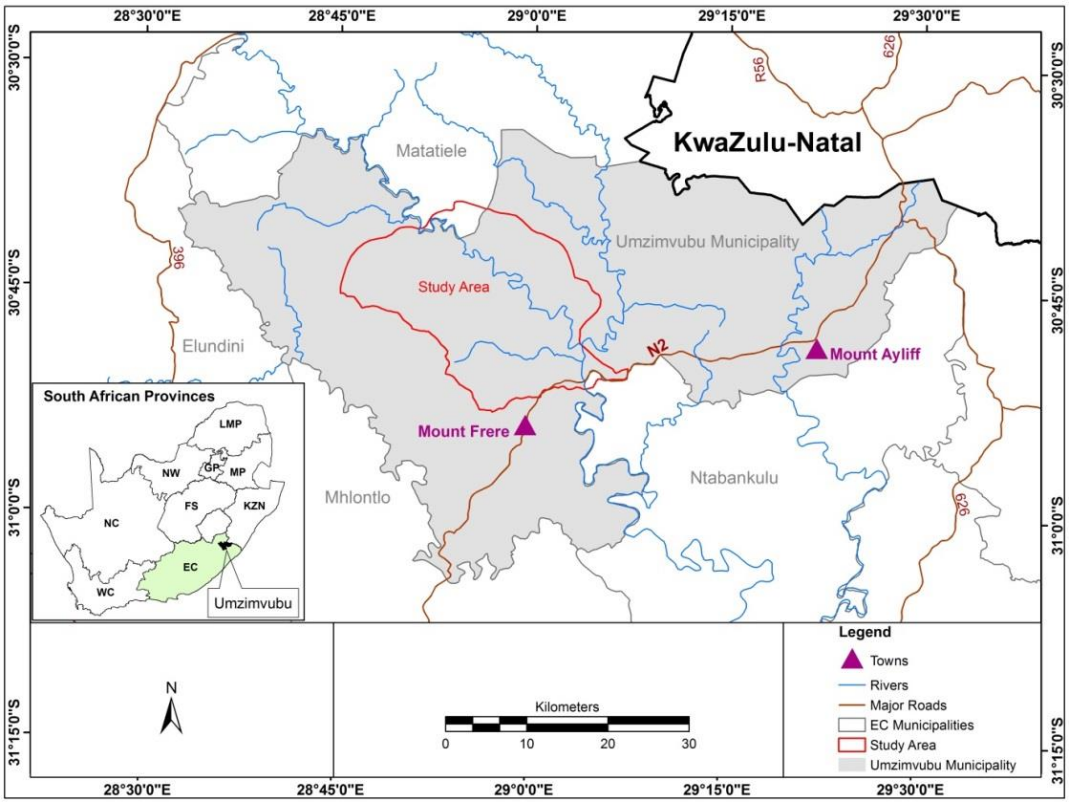

Figure 1. Location of the study area within the Umzimvubu Local Municipality.

3. Materials and Methods

3.1 Materials

The image data used in this study include Landsat8 Operational Land Imager (OLI) and *Satellites Pour l'Obsevation de la Terre* (SPOT6/7) multispectral images obtained in slightly different acquisition dates. The term "SPOT6/7" which will be used throughout this paper refers to a newly launched SPOT image product which combines the capabilities of SPOT6 and SPOT7 imagery. Landsat8 OLI consists of nine multispectral bands with a spatial resolution of 30m for bands 1 to 7 and 9. Band 8 (panchromatic) has a spatial resolution of 15m whereas bands 10 and 11 (thermal bands) are collected at 100m spatial resolution. SPOT6/7 consists of four multispectral bands with a spatial resolution of 6m and a panchromatic band with a spatial resolution of 1.5m. Landasat8 OLI was acquired in 2014-07-20 at 07:57:13 whereas SPOT6/7 was acquired in 2014-06-09 at 07:49:31 according to their respective scene centre times. SPOT6/7 and Google Earth were used as ancillary Landsat8 data for ground truth purposes. Besides providing superior spatial resolution, Google Earth was chosen as a surrogate for field work, thereby avoiding travelling costs. SPOT6/7 and Landsat8 OLI were chosen because they are readily available free of charge, but most importantly because of their suitability for detecting erosion features (Taruvinga, 2008; Dube *et al.*, 2017). Moreover,

Seutloali *et al*. (2016) maintain that Landsat data has proven to be significant in examining soil erosion occurrence especially in instances where in-depth field work remains a challenging task.

Landsat8 OLI was freely downloaded from the United States Geological Survey (USGS) website, while SPOT6/7 data was freely obtained from the South African Space Agency (SANSA). The Red (band 4), and near-infrared (NIR) (band 5) of Landsat8 OLI were utilised to compute NDVI and SAVI. SARVI was generated from the Blue (band 2), Red, and NIR bands of Landsat8 OLI. In order to minimise the effects of soil variability and atmospheric noise on vegetation, a soil calibration factor of 0.5 was used for both SAVI and SARVI including a blue-band normalisation for the latter (Huete *et al*., 1988; Huete and Liu, 1994).

3.2 Pre-processing

Prior to the actual image processing, Landsat8 OLI and SPOT6/7 scenes were subset to the study area (catchment) in order to restrict analysis; thereby reducing time required for image processing (Campbell and Wynne, 2011). Both SPOT6/7 and Landsat8 OLI multispectral images were obtained already pre-processed by suppliers. However, in order to obtain maximum surface reflectance, Landsat8 digital numbers (DN) were converted to Top Of Atmosphere (TOA) reflectance using the radiometric rescaling coefficients provided in the Landsat8 product metadata file (MTL file). All calculations were performed using the "raster calculator" tool within the ArcMap 10.2 environment. The following equation [1] available in the USGS Landsat8 website was used to convert digital numbers (DN) to TOA reflectance (Alhawiti and Mitsova, 2016):

$$\boldsymbol{\rho\lambda'} = \boldsymbol{M_\rho Q_{cal}} + \boldsymbol{A_\rho} \qquad [1]$$

Where $\boldsymbol{\rho\lambda'}$ is the TOA planetary reflectance (without correction for sola angle), $\boldsymbol{M_\rho}$ is the Band-specific multiplicative rescaling factor, $\boldsymbol{A_\rho}$ is the Band-specific additive rescaling factor, and $\boldsymbol{Q_{cal}}$ is the Quantized and calibrated standard product pixel values (DN).

Three Landsat8 OLI multispectral bands relevant to the computation of VIs, *viz*. Band 2 (Blue), Band 4 (Red), and Band 5 (NIR) were pan-sharpened to 15m spatial resolution using the panchromatic image (Band 8) of Landsat8 OLI. While various pan-sharpening algorithms have been proposed in the literature, the most widely used include Resolution Merge, Modified IHS (intensity hue saturation) Resolution Merge, and Adaptive IHS Pan-sharpening, amongst others (Rahmani *et al*., 2010; Zhang and Mishra, 2012). In this paper, the Resolution Merge pan-sharpening was considered based on the obtained output results relative to other algorithms that were tried and tested.

Pan-sharpening was conducted in ERDAS IMAGINE 2013 software using the built-in "Resolution Merge" module.

3.3 VIs Computation

The red and near-infrared (NIR) bands are probably the most important bands featured in all VIs calculations. This is so because vegetation reflects high in the near-infrared and low in the red band. By maximising this linear relationship between the red and NIR bands, VIs allow for sharp spectral discrimination between vegetation and non-vegetation attributes including soil erosion (Taruvinga, 2008). Given this linear relationship where soil erosion increases with decreasing vegetation (Seutloali and Beckedahl, 2015), an assumption can be made that areas lacking vegetation cover represents erosion, and would therefore exhibit a particular VI value or range (threshold) that could be used to identify eroded areas (Taruvinga, 2008). Furthermore, once erosion features are identified through a threshold technique, such erosion features can be mapped (Cyr *et al*., 1995). Other erosion-related studies that have applied threshold technique include that of Mathieu *et al.* (1997), Vaidyanathan *et al*. (2002), and Symeonakis and Drake (2004), amongst others. In this paper, a threshold technique is utilised in the subsequent section to classify soil erosion with the aid of each VI. While all VIs namely; NDVI, SAVI, and SARVI generally rely on red and NIR bands to calculate vegetation, they are computed using different formulas as indicated in equations [2], [3], and [4].

$$\boldsymbol{NDVI = \frac{R_{NIR} - R_{Red}}{R_{NIR} + R_{Red}}} \quad [2]$$

Where $\boldsymbol{R_{NIR}}$ is the near-infrared radiation, and $\boldsymbol{R_{Red}}$ is the visible red radiation.

$$\boldsymbol{SAVI = \frac{R_{NIR} - R_{Red}}{R_{NIR} + R_{Red+L}}(1 + L), L = 0.5} \quad [3]$$

Where $\boldsymbol{R_{NIR}}$ is the near-infrared radiation, $\boldsymbol{R_{Red}}$ is the visible red radiation, and L is the soil adjustment factor. An L value of 0.5 minimises the effects of soil brightness variations and eliminates the need for additional calibration for different soils (Huete and Liu, 1994).

$$\boldsymbol{SARVI = \frac{R_{NIR} - R_{RB}}{R_{NIR} + R_{RB+L}}(1 + L), L = 0.5} \quad [4]$$

Where $\boldsymbol{R_{RB}}$ is $\boldsymbol{R_R - \gamma(R_B - R_R)}$, $\boldsymbol{R_{NIR}}$ is the near-infrared radiation, $\boldsymbol{R_R}$ is the visible red radiation, and $\boldsymbol{R_B}$ is the visible blue radiation, L is the soil adjustment factor. Huete and Liu (1994) combined the soil adjustment factor (L) and a blue-band normalisation to correct for both soil and atmospheric noise.

3.4 Soil Erosion Classification.

Three VIs including NDVI, SAVI, and SARVI were produced mainly for soil erosion classification within the study area. All VIs were generated in ERDAS IMAGINE 2013 using predetermined formulas. The "arbitrary profiler" (spatial profiler) tool in ENVI5.2 was used to extract soil erosion reflectance values from selected gullies within the study area. Using a procedure similar to that of Taruvinga (2008) and Gandhi *et al*. (2015), best thresholds for soil erosion classification were determined for each VI on a trial and error basis. The benchmark used to select the best threshold was determined based on the accuracy of the derived erosion maps (i.e. overall accuracy and kappa statistics results). Raster calculator in ArcMap10.2 was then used to classify eroded areas based on the selected classification thresholds for each VI.

3.5 Accuracy Assessment

One of the simplest and yet widely accepted ways of assessing accuracy is to compare ground reference test data with remote sensing classification maps (Jensen, 2005). Integral to this, is obtaining the appropriate number of unbiased ground reference points. In this study, 100 random sample points were created using a "Create Random Points" tool in ArcMap 10.2. Within the "Create Random Points" tool dialogue box, the "Constraining Feature Class" option was set to the polygon shapefile of the study area in order to restrict random points within the boundaries of the study area. It is very important to collect ground reference test information as close to the date of image acquisition as possible (Jensen, 2005; Campbell and Wynne, 2011). Accordingly, high resolution and most recent images of SPOT6/7 (2014) and Google Earth image (2013) were used for ground truth to assess the accuracy of the 2014 Landsat classified images. The GIS-derived random points were initially converted to kml (keyhole makeup language) and exported to Google Earth for ground truth purposes. Given that soil erosion features are very small and often linear in shape, most of the random points were widely distributed on non-erosion features, with very few sitting on erosion features. Therefore, each random point was assigned to the adjacent erosion feature on Google Earth and these totalled to 40 while the remaining 60 random points sat on non-erosion features.

Confusion matrix was tabulated for each VI. Four levels of accuracy including user's accuracy, producer's accuracy, overall accuracy, and kappa statistics were calculated. Confusion matrix was chosen because it is one of the most widely used and accepted ways of expressing classification accuracy (Story and Congalton, 1986; Lillesand and Kiefer, 2000; Sonawane and Bhagat, 2017). The confusion matrix helped to examine the relationship between known reference data and the corresponding results of VI-derived maps.

4. Results and Discussion

4.1 Vegetation Indices Results

Figure 2 displays NDVI (a), SAVI (b), and SARVI (c) in a grey scale colour, where the white colour represents highly vegetated areas while the light grey colour denotes sparsely vegetated areas. The dark grey and black colours on the other hand, represent non-vegetated areas including water bodies, cultivated land, bare surfaces, and built-up areas, among others. SARVI (c) generally reflects higher than NDVI (a) and SAVI (b). As shown in Figure 2, the reflectance values for SARVI range from -0.82 to 0.96 with negative values representing water bodies and shadows. High positive values such as 0.96 denote areas of strong vegetation, for example, forests in this case. SAVI on the other hand closely follows SARVI with the minimum and maximum reflectance values of -0.84 and 0.93, respectively. Of all the indices, NDVI has the least reflectance values ranging from -0.77 to 0.84. While all three VIs provide a very sharp spectral contrast between vegetated and non-vegetated surfaces, most non-vegetation classes have low spectral contrast relative to one another. This is particularly the case in SARVI (c), where the spectral reflectivity of water bodies and most linear features such as roads and some gullies is almost the same; for example, they are all represented by a black colour. It is therefore possible to infer that although commands the highest spectral reflectivity; SARVI poorly discriminates among non-vegetation features at least in relation to other VIs.

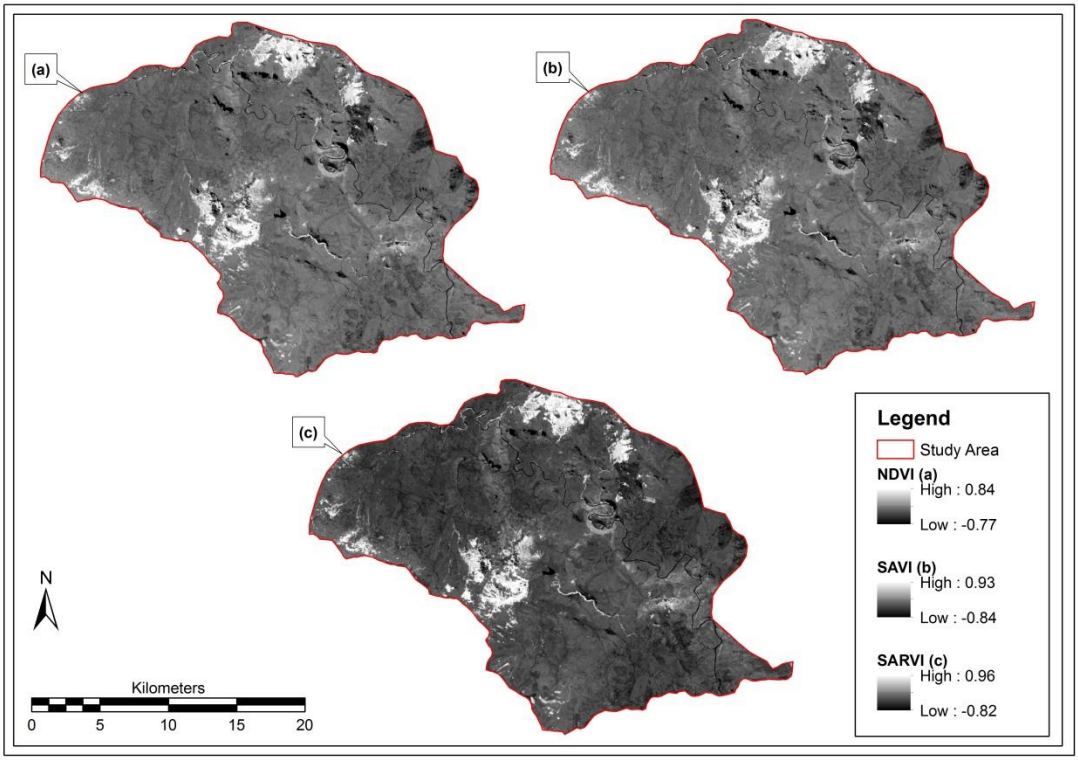

Figure 2. Vegetation indices: NDVI (a), SAVI (b), and SARVI (c).

4.2 Soil Erosion Classification from VIs

After a series of trial runs, 0.12 to 0.22 reflectance values were selected as the best threshold to classify soil erosion in NDVI while 0.15 to 0.25 and 0.13 to 0.22 were chosen for SAVI and SARVI, respectively. The "Raster Calculator" tool in ArcMap10.2 was used to classify erosion features based on the above-mentioned thresholds. Shown in Figure 3 are classification results of Landsat8 images based on the selected threshold reflectance values for each VI. The distribution of soil erosion is overlaid on SPOT6/7 imagery (Figure 4).

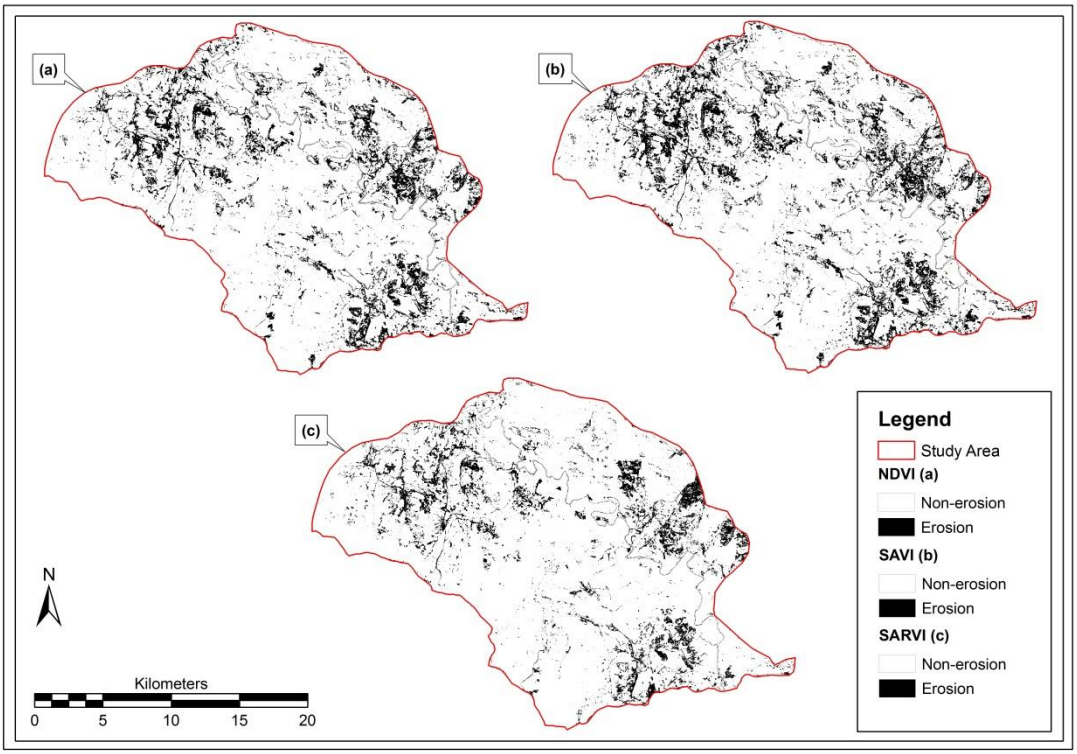

Figure 3. Soil erosion maps: NDVI (a), SAVI (b), and SARVI (c), classified from the Landsat8 OLI-derived VIs.

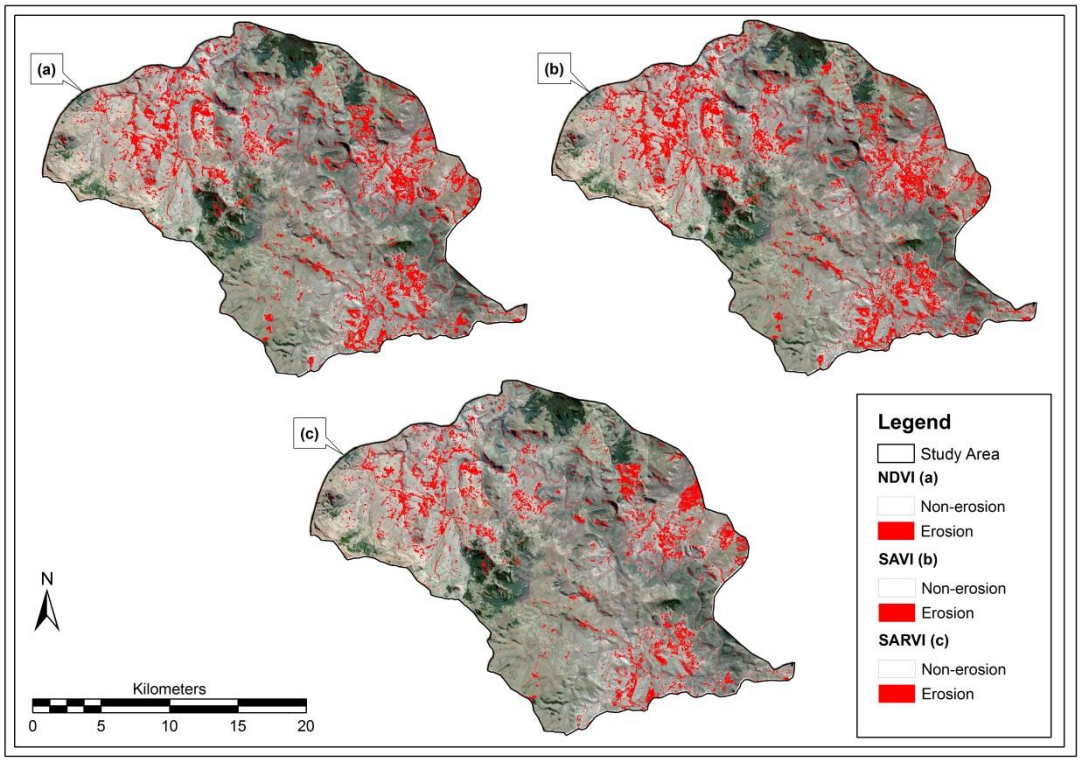

Figure 4. VI-classified soil erosion maps overlaid on SPOT6/7 imagery.

4.3 Accuracy Assessment Results of VI-derived Maps

A necessary step after remote sensing image classification is the accuracy assessment of the results. Table 1 provides the accuracy assessment report of VI-derived classification results with respect to producer's and user's accuracy along with overall accuracy and kappa statistics for erosion and non-erosion classes. Figure 5 provides a summary of the overall accuracy and kappa statistics.

The results indicate that NDVI achieved highest accuracy for producer's accuracy (78.4%) in the erosion class (Table 1). SAVI outperformed other VIs with an overall accuracy of 83% and kappa statistics of 0.64 (64%). NDVI and SARVI yielded the same results in terms of overall accuracy with slightly different kappa statistical results *viz*. 0.60 (60%) for the former and 0.59 (59%) for the latter. Relative to other VIs, SARVI recorded the lowest producer's accuracy of 62.5% and a commanding 86.7% user's accuracy for the erosion category. Since SAVI achieved the highest overall accuracy and kappa statistic results (Figure 5), it was chosen to classify soil erosion within the study area. Figure 6 shows the distribution of soil erosion over the entire study area while Figure 7 is zoomed in to the western portion of the study area.

Table 1. Accuracy assessment report for erosion and non-erosion classes in VIs.

	NDVI (%)		**SAVI (%)**		**SARVI (%)**	
Class	Erosion	No-erosion	Erosion	No-erosion	Erosion	No-erosion
Producer's accuracy	78.4	82.5	77.5	86.7	62.5	93.3
User's accuracy	73.0	86.7	79.5	85.2	86.2	78.9
Overall accuracy	**81.0**		**83.0**		**81.0**	
Kappa statistics	**0.60 (60%)**		**0.64 (64%)**		**0.59 (59%)**	

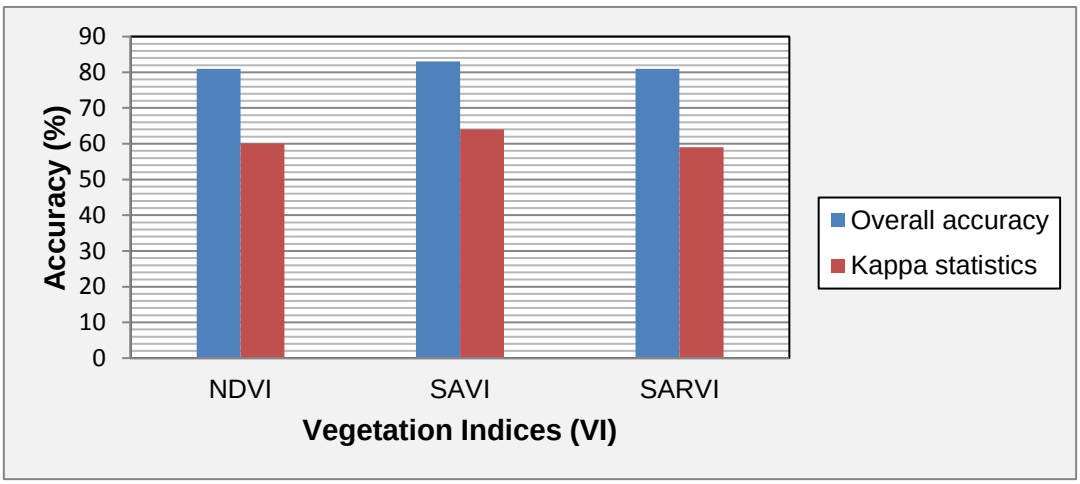

Figure 5. Summary statistical results of overall accuracy and kappa statistics.

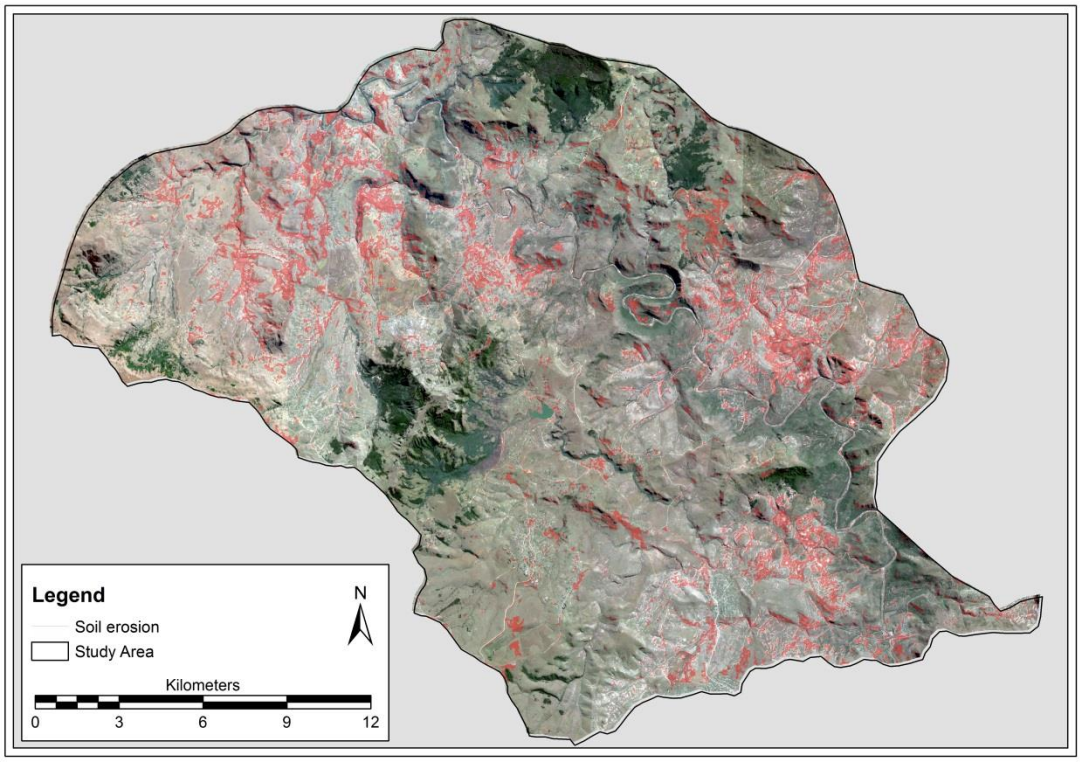

Figure 6. Soil erosion classified from SAVI, overlaid on SPOT6/7 imagery.

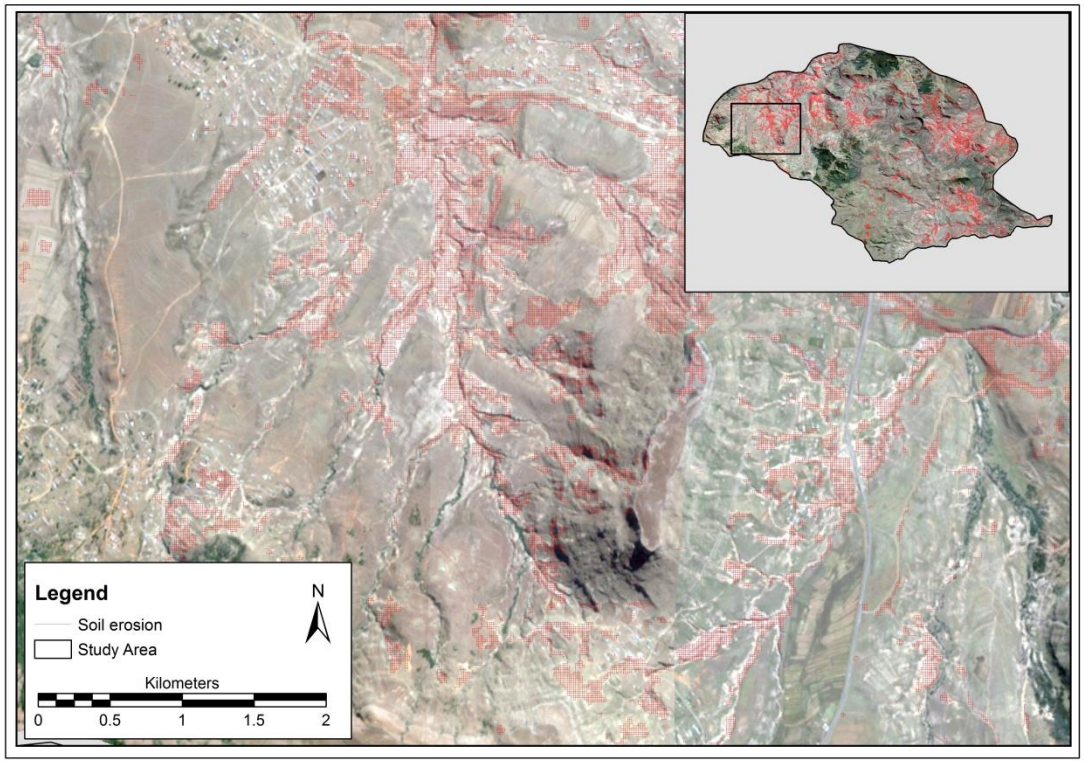

Figure 7. Soil erosion distribution in the western section of the study area.

4.4 Discussion

One objective of this study was to map the spatial distribution of soil erosion using three Landsat-derived VIs. Notwithstanding the success of the study in mapping the spatial distribution of soil erosion, the results ought to be examined from its proper perspective. Despite an attempt to improve the spatial resolution, not all soil erosion features have been classified, for example rills, sheet and some small gullies have been excluded possibly because their sizes fall below the spatial resolution (15m) of the pan-sharpened Landsat8 OLI. Within the study area, the spectral reflectivity of soil erosion varies considerably, and in some cases tends to be similar to non-erosion features (for example bare soil). The possibility therefore exists that some soil erosion features may have been classified as non-erosion features. For example, the spectral reflectance of sheet erosion resembles that of bare soil surfaces making it difficult if not impossible to spectrally discriminate between the two features. Admittedly, an overall accuracy of 83% for SAVI and 81% for NDVI and SARVI denotes a good or perhaps high level of accuracy (Taruvinga, 2008; Mararakanye and Nethengwe, 2012; Sonawane and Bhagat, 2017). However, these may be misleading as well, given that much of the study area is covered by the non-erosion features, for instance; at least 80% of the study area in each VI, constitutes non-erosion features. Accordingly, using an overall accuracy as a proxy of accuracy could be very biased because of the larger spatial coverage of the non-erosion class (Taruvinga, 2008).

In the confusion matrix (Table 1), all VIs generally exhibit high producer's or user's accuracies for non-erosion class, while the erosion category records comparatively low accuracies from both the producer's and user's perspective. For example, SAVI has producer's accuracy of 86.7% and 77.5% for non-erosion and erosion categories, respectively (Table 1), whereas user's accuracy is 85.2% for the non-erosion and 79.5% for the erosion class. The same applies for NDVI and SARVI. Conversely, of all the indices, SARVI (Table 1) records better results, at least from the user's point of view (86.2%), albeit the overall accuracy of 81% and kappa statistic of 0.59 (59%) are undeniably poor results. The SAVI-derived erosion map on the other hand records quite good results across all levels of accuracy, including the producer's and user's accuracy of 77.5% and 79.5% for the erosion class, respectively, together with kappa statistical results of 0.64 (64%).

Another objective of this study was to test the accuracy of VI-derived maps and determine the best VI for mapping soil erosion features at a scale of the study *viz*. catchment scale. Based on accuracy results, particularly kappa statistics, it is apparent that SAVI is the best VI for detecting soil erosion features at a catchment scale and a spatial resolution of 15m. While the kappa statistics of 0.64 (64%)

for SAVI, 0.60 (60%) for NDVI, and 0.59 (59%) for SARVI do not represent a strong agreement (i.e. kappa statistic > 0.80) between the classified erosion on the maps and corresponding erosion on the real ground (Jensen, 2005), these results represent moderate agreement (i.e. kappa statistic > 0.40 to 0.80) (Landis and Koch, 1977 in Jensen, 2005) which is adequate and acceptable for identifying soil erosion features at a catchment level. For example, the study by Mararakanye and Nethengwe (2012) produced kappa statistics of 0.52 (52%) while Taruvinga (2008) yielded kappa statistics of 0.555 (56%), 0.496 (50%), and 0.5580 (56%) for NDVI, SAVI and TSAVI, respectively; and were all considered moderately accurate and valid.

5. Conclusion and Recommendations `

Overall, this study successfully mapped the spatial distribution of soil erosion in a quaternary catchment within the Umzimvubu Municipality in Eastern Cape, South Africa. The kappa statistical results of 0.64 for SAVI, 0.60 for NDVI, as well as 0.59 for SARVI which are all considered acceptable and valid, justify this conclusion. Relative to other indices, it has been proven that SAVI is the most suitable VI for mapping soil erosion at a catchment level. Despite these positive results, the detection of some small erosion features proved to be a challenge in this study partly because of the coarser spatial resolution (15mx15m) of Landsat8 OLI. This challenge was further compounded by the spectral homogeneity of soil erosion and non-erosion features. It is therefore highly recommended that soil erosion studies use alternative methods related to pan-sharpening and fusion of Landsat8 with panchromatic or multispectral data of higher spatial resolution images such as SPOT, QuickBird, IKONOS, and WorldView images amongst others. One way to improve the detection and spectral discrimination of erosion features is to integrate spectral and textural information through object-based image classification. Previous studies have shown that land managers and policy makers are more interested in the spatial distribution of soil erosion than in absolute values of soil loss (Lu *et al*., 2004). Therefore, this study sheds light not only on the spatial distribution of soil erosion in the study area but also provides a useful framework for land managers and decision makers when planning soil erosion management at the catchment level.

6. Acknowledgement

The authors would like to thank the United States Geological Survey (USGS) and the South African Space Agency (SANSA) for providing free Landsat and SPOT data respectively.

7. References

Aiello, A., Adamo, M & Canora, F 2015, 'Remote sensing and GIS to assess soil erosion with RUSLED and USPED at river basin scale in southern Italy', *Catena*, vol. 131, pp. 174-185.

Alexakis, DD., Hadjimitsis, DG & Agapiou, A 2013, 'Integrated use of remote sensing, GIS and precipitation data for the assessment of soil erosion rate in the catchment area of "Yialias" in Cyprus', *Atmospheric Research*, vol. 131, pp. 108-124.

Alhawitti, RH & Mitsova, D 2016, 'Using Landsat-8 data to explore the correlation between urban heart island and urban land uses', *IJRET: International Journal of Research in Engineering and Technology*, vol. 5, no. 3, pp. 457-466.

Beckhedahl, HR & De Villiers, AB 2000, 'Accelerated erosion by piping in the Eastern Cape Province, South Africa', *South African Geographical Journal*, vol. 82, no. 3, pp. 157-162.

Boardman, J., Parsons, AJ., Holland, R., Holmes, PJ & Washington, R 2003, 'Development of badlands and gullies in the Sneeuberg, Great Karoo, South Africa', *Catena*, vol. 50, no. 2-4, pp. 165-184.

Campbell, JB & Wynne, RH 2011, *Introduction to remote sensing*, 5th edition, The Guilford Press, New York.

Cyr, L., Bonn, F & Pesant, A 1995, 'Vegetation indices derived from remote sensing for an estimation of soil protection against water erosion', *Ecological Modelling*, vol. 79, no. 1-3, pp. 277-285.

Dube, T., Mutanga, O., Sibanda, M., Seutloali, K & Shoko, C 2017, 'Use of Landsat series data to analyse the spatial and temporal variations of land degradation in a dispersive soil environment: A case of King Sabata Dalindyebo local municipality in the Eastern Cape Province, South Africa', *Physics and Chemistry of the Earth*, viewed 06 April 2017<https://doi.org/10.1016/j.pce.2017.01.023>.

Ganasri, BP & Ramesh, H 2015, 'Assessment of soil erosion by RUSLE model using remote sensing and GIS – A case study of Nethravathi Basin', *Geoscience Frontiers*, vol. 7, no. 6, pp. 953-961.

Gandhi, MG., Parthiban, S., Thummalu, N & Christy, A 2015, 'Ndvi: Vegetation change detection using remote sensing and gis – A case stdudy of Vellore District', *Procedia Computer Science*, vol. 57, pp. 1199-1210.

Garland, GG., Hoffman, MT & Todd, S 2000, 'Soil degradation', in MT Hoffman, S Todd, Z Ntshona & S Turner (eds.), *A national review of land degradation in South Africa*, University of Cape Town, Plant Conservation Unit, Cape Town, viewed 05 April 2016, <http://www.pcu.uct.ac.za/search/?cx=002153019866612815917:odspxe3g6c0>.

Govaerts, B & Verhulst, N 2010, *The Normalised Difference Vegetation Index (NDVI) GreenSeeker™ handhaeld sensor: toward the integrated evaluation of crop management*, viewed 10 April 2017, <http://plantstress.com/methods/Greenseeker.PDF>.

Huete, AR & Liu, HQ 1994, 'An error and sensitivity analysis of the atmosphere- and soil-correcting variants of the NDVI for the MODIS-EOS', *IEEE Transections on Geoscience and Remote Sensing*, vol. 32, no. 4, pp. 897-905.

Huete, AR 1988, 'A Soil Adjusted Vegetation Index (SAVI)', *Remote Sensing of Environment*, vol. 25, no. 3, pp. 295-309.

Jensen, JR 2005, *Introductory digital image processing: a remote sensing perspective*, 3rd edition, Pearson Prentice Hall, Chicago.

Jie, C., Jing-zheng, C., Man-zhi, T & Zhi-tong, G 2002, 'Soil degradation: a global problem endangering sustainable development', *Journal of Geographical Science*, vol. 12, no. 2, pp. 243-252.

Kinnell, PIA 2010, 'Event soil loss, runoff and the Universal Soil Loss Equation family of models: A review', *Journal of Hydrology*, vol. 385, no. 1-4, pp. 384-397.

Lawrence, RL & Ripple, WJ 1998, 'Comparison among vegetation indices and banwise regression in a highly disturbed heterogeneous landscape: Mount St. Helens, Washington', *Remote Sensing of Environment*, vol. 64, no. 1, pp. 91-102.

Le Roux, JJ & Sumner, PD 2012, 'Factors controlling gully development: Comparing continuous and discontinuous gullies', *Land Degradation and Development*, vol. 23, no. 5, pp. 440-449.

Le Roux, JJ., Morgenthal, TL., Malherbe, J., Sumner, PD & Pretorius, DJ 2008, 'Water erosion prediction at a national scale for South Africa', *Water SA*, vol. 34, no. 3, pp. 305-314.

Le Roux, JJ., Newby, TS & Sumner, PD 2007, 'Monitoring soil erosion in South Africa at a regional scale: review and recommendations', South *African Journal of Science*, vol. 103, no. 7-8, pp. 329-335.

Lillesand, TM & Kiefer RW 2000, *Remote sensing and image interpretation*, 4th edition, John Wiley & Sons, New York.

Lu, D., Li, G., Valladares, GS & Batistella, M 2004, 'Mapping soil erosion in Rondônia, Brazilian Amazonia: Using RUSLE, remote sensing and GIS', *Land Degradation and Development*, vol. 15, no. 5, pp. 499-512.

Macharia, SN 2005, 'New directions for coastal and marine monitoring: web mapping and mobile application technologies', in D Bartlett & J Smith (eds.), *GIS for coastal zone management*, CRC Press, Boca Raton.

Madikizela, PNT 2000, *Spatial and temporal aspects of soil erosion in MT Ayliff and MT Frere, Eastern Cape Province*, South Africa, Petermaritzburg, University of Natal, MSc thesis.

Mararakanye, N & Nethengwa, NS 2012, 'Gully features extraction using remote sensing techniques', *South African Journal of Geomatics*, vol. 1, no. 2, pp. 109-118.

Mathieu, R., King, C & Le Bissonnais, Y 1997, 'Contribution of multi-temporal SPOT data to the mapping of a soil erosion index: the case of the loamy plateau of northern France', *Soil Technology*, vol. 10, no. 2, pp. 99-110.

Mayr, A., Rutzinger, M., Bremer, M & Geitner, C 2016, 'Mapping eroded areas on mountain grassland with terrestrial photogrammetry and object-based image analysis', *ISPRS Annals of the Photogrammetry, Remote Sensing and Spatial Information Sciences*, vol. 3-5, viewed 30 April 2017, <http://www.isprs-ann-photogramm-remote-sens-spatial-inf-sci.net/III-5/137/2016/isprs-annals-III-5-137-2016.pdf>.

Merrite, WS., Letcher, RA & Jakeman, AJ 2003, 'A review of erosion and sediment transport models', *Environmental Modelling & Software*, vol. 18, no. 8-9, pp. 761-799.

Ngetar, SN 2011, *Causes of wetland erosion at Craigieburn, Mpumalanga Province, South Africa*, Durban, South Africa, University of KwaZulu-Natal, PhD thesis.

Oldeman, LR., Hakkeling, RTA & Sombroek, WG 1991, *World map of the status of human induced soil degradation: An explanatory note*, ISRIC, Wageningen.

Owusu, O 2012, 'A GIS-based estimation of soil loss in the Densu Basin in Ghana', *West African Journal of Applied Ecology*, vol. 20, no. 2, pp.41-52.

Pimentel, D 2006, 'Soil erosion: a food and environmental threat', *Environment, Development and Sustainability*, vol. 8, no. 1, pp. 119-137.

Rahmani, S., Strait, M., Merkurjev, D., Moeller, M & Wittman, T 2010, 'An adaptive IHS pan-sharpening method', *IEEE Geoscience and Remote Sensing Letters*, vol. 7, no. 4, pp. 746-750.

Rouse, JW., Haas, RH., Schell, JA & Deering, DW 1973, 'Monitoring vegetation systems in the Great Plains with ERTS', in *3rd ERTS Symposium*, NASA, Washington DC.

Scherr, SJ & Yadav, S 1997, *Land degradation in the developing world: policy issues and options* viewed 10 April 2017, <http://ageconsearch.umn.edu/bitstream/16371/1/br44.pdf>.

Seutloali, KE & Beckedahl, HR 2015, 'Understanding the factors influencing rill erosion on roadcuts in the south eastern region of South Africa' *Solid Earth*, vol. 6, no. 2, pp. 633-641.

Seutloali, KE., Beckedahl, HR., Dube, T & Sibanda, M 2015, 'An assessment of gully erosion along major armoured roads in south-eastern South Africa: a remote sensing and GIS approach', *Geocarto International*, vol. 31, no. 2, pp. 225-239.

Seutloali, KE., Dube, T & Mutanga, O 2016, 'Assessing and mapping the severity of soil erosion using the 30-m Landsat multispectral satellite data in the former South African homelands of Transkei', *Physics and Chemistry of the Earth*, viewed 06 April 2017, <https://doi.org/10.1016/j.pce.2016.10.001>.

Shruthi, RBV., Kerle, N & Jetten, V 2011, 'Object-based gully feature extraction using high resolution imagery', *Geomorphology*, vol. 134, no. 3-4, pp. 260-268.

Singh, D., Herlin, I., Berroir, JP., Silva, EF & Simoes, MM 2004, 'An approach to correlate NDVI with soil colour for erosion process using NOAA/AVHRR data', *Advances in Space Science Research*, vol. 33, no. 3, pp. 328-332.

Sonawane, KR & Bhagat, VS 2017, 'Improved change detection of forests using Landsat TM and ETM+ data', *Remote Sensing of Land*, vol. 1, no. 1, pp. 18-40.

Story, M & Congalton, RG 1986, 'Accuracy assessment: a user's perspective', *Photogrammetric Engineering and Remote Sensing*, vol. 52, no. 3, pp. 397-399.

Symeonakis, E & Drake, N 2004, 'Monitoring desertification and land degradation over sub-Saharan Africa', *International Journal of Remote Sensing*, vol. 25, no. 3, 573-592.

Taruvinga, K 2008, *Gully mapping using Remote Sensing: Case study in KwaZulu-Natal, South Africa*. Ontario, Canada, University of Waterloo, MSc thesis.

Vaidyanathan, NS., Sharama, G., Sinha, R & Dikshit, O 2002, 'Mapping of erosion intensity in the Garhwali Himalaya', *International Journal of Remote Sensing*, vol. 23, no. 20, pp. 4125-4129.

Wischmeier, WH & Smith, DD 1965, 'Predicting rainfall erosion from cropland east of the Rocky Mountain: Guide for selection of practices for soil and water conservation'. *Agricultural Handbook No. 537*, U.S. Department of Agriculture.

Zhang, Y & Mishra, RK 2012, *A review and comparison of commercially available pan-sharpening techniques for high resolution satellite image fusion*, viewed 04 April 2017, <http://ieeexplore.ieee.org/stamp/stamp.jsp?arnumber=6351607&tag=1>.